Naval Research Laboratory

Washington, DC 20375-5320

NRL/MR/6355--15-9581

Effect of Sensitization on Corrosion-Fatigue Cracking in Al 5083 Alloy

P.S. Pao
R.L. Holtz
R. Goswami

Multifunctional Materials Branch
Materials Science and Technology Division

R.A. Bayles

Center for Corrosion Science and Engineering
Chemistry Division

January 21, 2015

REPORT DOCUMENTATION PAGE

Form Approved
OMB No. 0704-0188

1. REPORT DATE *(DD-MM-YYYY)*	**2. REPORT TYPE**	**3. DATES COVERED** *(From - To)*
21-01-2015	Memorandum Report	October 2011 – September 2014

4. TITLE AND SUBTITLE

Effect of Sensitization on Corrosion-Fatigue Cracking in Al 5083 Alloy

5a. CONTRACT NUMBER

5b. GRANT NUMBER

5c. PROGRAM ELEMENT NUMBER

6. AUTHOR(S)

P.S. Pao, R.L. Holtz, R. Goswami, and R.A. Bayles

5d. PROJECT NUMBER

5e. TASK NUMBER

5f. WORK UNIT NUMBER
63-2634-A4

7. PERFORMING ORGANIZATION NAME(S) AND ADDRESS(ES)

Naval Research Laboratory
4555 Overlook Avenue, SW
Washington, DC 20375-5328

8. PERFORMING ORGANIZATION REPORT NUMBER

NRL/MR/6355--15-9581

9. SPONSORING / MONITORING AGENCY NAME(S) AND ADDRESS(ES)

Office of Naval Research
One Liberty Center
875 North Randolph Street, Suite 1425
Arlington, VA 22203-1995

10. SPONSOR / MONITOR'S ACRONYM(S)

ONR

11. SPONSOR / MONITOR'S REPORT NUMBER(S)

12. DISTRIBUTION / AVAILABILITY STATEMENT

Approved for public release; distribution is unlimited.

13. SUPPLEMENTARY NOTES

14. ABSTRACT

An investigation was carried out to characterize the effect of sensitization (or aging), environment (including [NaCl] concentration), and load ratio on fatigue crack growth and stress-corrosion cracking (SCC) of Al 5083 alloy. Both low and high load ratios, corresponding to R = 0.1 and R = 0.85 were examined. The results indicate: (1) fully sensitized Al 5083 has very low high stress-ratio (at R = 0.85) corrosion-fatigue (CF) threshold stress intensity (ΔK_{th}) and SCC threshold (K_{1SCC}) in saltwater; (2) the as-received Al 5083-H131 has good CF and SCC resistance; (3) at 175°C aging temperature, high stress ratio ΔK_{th} and K_{1SCC} in saltwater decrease with increasing aging time up to about 240 hours; aging times longer than 240 hours produce little additional degradation; (4) sensitization has no effect on fatigue crack growth at low stress ratio of R = 0.1 in any environment, and no effect at any stress ratio in vacuum and in ambient air; (5) both high stress ratio ΔK_{th} and K_{1SCC} are influenced by [NaCl] concentration, higher [NaCl] results in a lower high stress ratio ΔK_{th} and K_{1SCC}.

15. SUBJECT TERMS

Corrosion-fatigue
Stress-corrosion cracking
Aluminum alloys
Sensitization

16. SECURITY CLASSIFICATION OF:			**17. LIMITATION OF ABSTRACT**	**18. NUMBER OF PAGES**	**19a. NAME OF RESPONSIBLE PERSON**
a. REPORT	**b. ABSTRACT**	**c. THIS PAGE**			Peter S. Pao
Unclassified Unlimited	Unclassified Unlimited	Unclassified Unlimited	Unclassified Unlimited	35	**19b. TELEPHONE NUMBER** *(include area code)* (202) 767-0224

Contents

ACKNOWLEDGMENTS

The authors gratefully acknowledge the support from Office of Naval Research (ONR), Arlington, VA, monitored by Dr. Lawrence Kabacoff. The authors wish to express their appreciation to Dr. A.K. Vasudevan, formerly with ONR, for his helpful discussions, to Dr. C.R. Feng for his assistance in SEM fractographic examination, and to Dr. F. Bovard of Alcoa for providing Al 5083-H131 plates.

INTRODUCTION

Aluminum alloy 5083-H131 is an armor-grade aluminum alloy that is non-heat-treatable and derives its strength from magnesium solute hardening and strain hardening. This alloy has good strength-to-weight ratio, weldability, and corrosion resistance in marine environments and has been used in ship structures and amphibious vehicles. However, Al 5083 is susceptible to intergranular corrosion and stress-corrosion cracking (SCC) when this alloy is exposed to elevated temperature (above 50 °C) for a prolonged period of time. The cause of SCC cracking has been attributed to the formation of grain boundary β phase (Al_3Mg_2) upon aging ("sensitization") at elevated temperatures for a long time (references 1-11). The presence of β phase is detrimental to the alloy's SCC resistance because β is electrochemically more active than the surrounding aluminum matrix and, thus, will dissolve preferentially in marine environments (references1-2). Even though the damaging effect of grain boundary β and sensitization on SCC in 5xxx-series aluminum alloys is well known, the effect of grain boundary β on the crack growth of Al 5083 under cyclic loading conditions in general and high stress-ratio corrosion fatigue in particular has not been systematically investigated.

In this study, the high stress-ratio (R = minimum load/maximum load = 0.85) corrosion fatigue crack growth and stress-corrosion cracking of Al 5083 subjected to various degrees of sensitization (from as-received condition to partially sensitized to fully sensitized) are determined and are correlated to the underlying grain boundary microstructure. The results are compiled into this report.

EXPERIMENTAL PROCEDURE

The material used in this study was 58.4-mm thick 5083-H131 plate. The specimens were sensitized at 175 °C for between 1 to 5000 hours. The Al 5083 plates have nominal chemical composition of Mg: 4.4 %, Mn: 0.7 %, Cr: 0.15 %, Si: max 0.4 %, Fe: max 0.4 %, Cu: max 0.1 %, Zn: max 0.25 %, Ti: max 0.15%, and Al: balance. The typical yield strength for Al 5083-H131 is 241 MPa.

For fatigue crack growth and stress-corrosion cracking studies, S-L oriented 12.7-mm-thick, 58.4-mm-wide wedge-opening-load (WOL) fracture mechanics specimens were used. That is, the crack propagation direction was parallel to the rolling direction and the crack plane is the plate's parting plane. The stress-intensity factor range (ΔK) for the WOL specimens was computed from the relationship (reference 12):

$$\Delta K = [\Delta P/(BW^{1/2})]\,[(2 + a/W)(0.8072 + 8.858\,(a/W) - 30.23\,(a/W)^2 + 41.088\,(a/W)^3 - 24.15\,(a/W)^4 + 4.951\,(a/W)^5]/(1 - a/W)^{3/2}, \quad (1)$$

where ΔP = applied load amplitude, B = specimen thickness, W = specimen width, and a = crack length. The fatigue test environments include vacuum (< 6 x 10^{-6} Pa background pressure), ambient air (20 °C and 42% relative humidity), and in saltwater solution with [NaCl] concentration varies from 0.001 to 15 wt%. For saltwater fatigue crack growth and stress-corrosion cracking experiments, a corrosion inhibitor (0.02 M $Na_2Cr_2O_7$, 0.07

Manuscript approved October 28, 2014.

M $MaC_2H_3O_2$, and $HC_2H_3O_2$ to pH 4) is added to prevent the crack tip corrosion product forming and the associated corrosion product induced wedging phenomenon. The fatigue crack growth experiments were conducted in accord with ASTM E647 with a cyclic load frequency of 10 Hz, a sine waveform, and load ratios, R, ranging from 0.1 to 0.8. Fatigue crack length and fatigue crack growth rate were continuously monitored by a compliance technique. For saltwater stress-corrosion cracking experiments, a step load test technique with a 10-hour hold time between each step was used. After fatigue and stress-corrosion cracking tests, the fatigue-fractured surfaces were studied by scanning electron microscopy (SEM).

RESULTS AND DISCUSSION

GRAIN BOUNDARY MICROSTRUCTURE

The effect of aging on the grain boundary microstructure has been extensively studied by Goswami, et al and has been published in the literature. The grain boundary microstructural evolution as aging progress has a significant effect on the corrosion-fatigue and stress-corrosion cracking resistance of Al 5083 and is briefly summarized below.

In as-received Al 5083-H131 the grain boundaries are mostly free of precipitates. Upon sensitization or aging at 175 °C, β phase (Al_3Mg_2) starts to form on the grain boundaries (as well as well as on Mn-rich dispersoids inside the matrix). The details of β phase evolution have been discussed previously (references 3-4). While β in the matrix will produce small corrosion pits, it is well known (references 1-2) that the β on the grain boundaries is significantly damaging as it can dissolve and facilitate cracking under SCC and corrosion fatigue conditions. Therefore, only the progress of β phase formation on the grain boundaries upon aging will be discussed here.

After 1-hour aging at 175 °C, discrete β precipitates start to form along the grain boundaries. These fine grain boundary β precipitates are several hundred nanometers in length and about 60 nanometers in width. Upon aging at 175 °C for 50 hours, the grain boundary β precipitates become more numerous, forming a ribbon-like morphology. These β precipitates are discontinuous and the grain boundary is not fully covered by β phase at this stage. Only after a long period of aging (greater than 240 hours), do β precipitates coalesce and the grain boundary becomes fully covered with a β film.

EFFECT OF SENSITIZATION ON FRACTURE TOUGHNESS

The effect of aging on fracture toughness of Al 5083 is shown in Fig. A-1. The aging effect on fracture toughness of Al 5083-H116 reported by Gao, et al was also included in Fig. A-1 for comparison. As shown in Fig. A-1, aging has only a slight effect on the fracture toughness as it ranges from 22 MPa√m for as-received Al 5083-H131 to 25 MPa√m for fully sensitized condition. The fracture toughness for Al 5083-H131 was measured according to ASTM E 399 guidelines (reference 13).

Though the fracture toughness reported by Gao, et al was significantly higher than that determined in this study, the general trend is similar as the fracture toughness increases initially upon aging and then reaches a maximum when material is fully sensitized, with no further increase in fracture toughness beyond this point. The reported higher fracture toughness probably is because the authors used a pop-in technique for precracking and far higher precracking stress intensity in their determination of the fracture toughness.

EFFECT OF SENSITIZATION ON FATIGUE CRACK GROWTH

The effects of aging on fatigue crack growth of Al 5083 at low stress ratio of R = 0.1 and high stress ratio of R = 0.85 in vacuum, ambient air, and 1% NaCl solution are shown in Figs. A-2a and A-2b, respectively. As shown in Fig. A-2, the fatigue crack growth rates and the fatigue crack growth thresholds (ΔK_{th}) for as-received and fully sensitized Al 5083 are comparable in vacuum and ambient air at either R = 0.1 or R = 0.85. In 1% NaCl solution and at R = 0.1, though the fatigue crack growth rates for fully sensitized Al 5083 are slightly higher (up to three times) than those for as-received alloy, the ΔK_{th} are essentially similar nevertheless. However, at R = 0.85 and in 1% NaCl solution, the fatigue crack growth rates of fully sensitized Al 5083 are about an order-of-magnitude higher that those of the as-received alloy. In addition, the ΔK_{th} of fully sensitized Al 5083 is less than one half of that of as-received alloy. That is the fatigue resistance of fully sensitized Al 5083 is at its worst under high stress ratio of R = 0.85 in 1% NaCl solution. Thus, in the subsequent fatigue studies, we are focusing only on the effects of sensitization and environment on high stress ratio corrosion fatigue crack growth at R = 0.85 in saltwater environments.

The corrosion-fatigue crack growth kinetics at a high stress ratio of R = 0.85 in 1% NaCl solution for as-received Al 5083-H131 and Al 5083 aged at 175 °C for 1 to 2000 hours are shown in Fig. A-3. As shown in Fig. A-3, the fatigue crack growth curve for each Al 5083 condition can be divided into a near-threshold Stage 1 and a power-law relation Stage 2. Because of high stress ratio and thus high mean stress intensity during the cyclic loading, Stage 3 fatigue crack growth, where crack growth transitions from Stage 2 to instability as the maximum stress intensity approaches the fracture toughness, is difficult to obtain and is not presented here.

The corrosion-fatigue crack growth rate is the lowest and ΔK_{th} is the highest in as-received Al 5083-H131, as shown in Fig. A-3. As the aging time at 175 °C increases from 1 to about 240 hours, the fatigue crack growth rates increase and ΔK_{th} decreases progressively. Such increase in fatigue crack growth rates and decrease in ΔK_{th} are illustrated in Figs. A-4 and A-5, respectively. As shown in Fig. A-5, the ΔK_{th} decreases linearly with increasing aging time at 175 °C from 1 to 240 hours.

At 240 hours aging, the ΔK_{th} reaches a minimum and is essentially unchanged upon further aging to 1000 hours. Similarly, as shown in Fig. A-4, the fatigue crack growth rate increases linearly with aging time up to 240 hours aging and reaches a maximum and remains unchanged from 240 to 1000 hours aging.

The observed corrosion-fatigue crack growth responses in Al 5083 subjected to various aging times at 175 °C, as shown in Figs. A-3 – A-5, correlate well to the grain boundary β phase formation. When the grain boundaries contain no β, as in the case of as-received Al 5083-H131, the corrosion-fatigue crack growth rate is the lowest and ΔK_{th} is the highest. As the aging proceeds at 175 °C, β starts to precipitate on the grain boundary, initially limited, discrete, and discontinuous for 1 hour aging, and β precipitates on the grain boundary become more numerous but still discontinuous for 50 hours aging. With such discontinuous grain boundary β morphology, the ΔK_{th} decreases and fatigue crack growth rate increases with the amount of β on the grain boundary. When Al 5083 is aged at 175 °C for more than 240 hours, grain boundaries are covered with continuous β film and ΔK_{th} reaches a minimum and fatigue crack growth rate reaches a maximum. Beyond 240 hours aging, the ΔK_{th} and fatigue crack growth rates both remain essentially unchanged as the grain boundaries are all covered with continuous β film.

EFFECT OF ENVIRONMENT

The effects of environment on fatigue crack growth of as-received and fully sensitized Al 5083-H131 at stress ratio R = 0.1 and 0.85 are shown in Figs. A-2a and A-2b. The test environments ranged from inert vacuum, ambient air, and 1% NaCl solution. As shown in Figs. A-2a and A-2b, irrespective of aging conditions and stress ratios, the fatigue crack growth rates are lowest in vacuum, followed by those in ambient air, and are highest in 1% NaCl. Depending on applied stress intensity, the fatigue crack growth rates in air are as much as two orders-of-magnitude higher than those from vacuum. The fatigue crack growth rates obtained in 1% NaCl are up to an order-of-magnitude higher than those in ambient air. Furthermore, the fatigue crack growth threshold stress intensity factor, ΔK_{th}, below which the crack will not grow, obtained in vacuum is significantly higher than those from ambient air and in 1% NaCl. It is interesting to note in Fig. A-2, although fatigue crack growth rates in 1% NaCl are higher than those from ambient air, the ΔK_{th} obtained in ambient air and in 1% NaCl are comparable at R = 0.1 for both as-received and fully sensitized Al 5083 and at R = 0.85 for only as-received Al 5083. As stated before, for fully sensitized Al 5083 at R = 0.85 and in 1% NaCl solution, the ΔK_{th} is significantly lower and fatigue crack growth rates are considerably higher than those obtained from ambient air.

Except for the case of fully sensitized Al 5083 at high stress ratio of R = 0.85 in 1% NaCl solution, the observed environmental effects on fatigue crack growth can be explained by the hydrogen embrittlement mechanism and are consistent with previous investigations (references 14-17). The water vapor in ambient air is known to react with freshly created aluminum fatigue fracture surfaces. The hydrogen thus generated from water vapor/aluminum reaction enters into fatigue crack tip region and accelerates fatigue crack growth and lowers ΔK_{th} via hydrogen embrittlement mechanism (references 14, 16, and 18). In saltwater environment, the same water/aluminum surface reaction produces hydrogen and enhances fatigue crack growth. It is speculated that, in the Stage 2 fatigue crack growth region, the complex electrochemical reactions occurring at the crack tip may enhance hydrogen entry and cause additional embrittlement and higher fatigue crack growth rates than those obtained in ambient air. In the near-threshold Stage 1 region,

where fatigue crack growth rates are slowest and the time for water/aluminum surface reactions are longest, it is speculated that the surface reactions in ambient air and in saltwater are saturated and comparable amount of hydrogen enters the crack tip region and, hence, the similar ΔK_{th} in ambient and in 1% NaCl.

As stated previously, the grain boundaries in fully sensitized Al 5083 are covered with a continuous β phase film. β phase is electrochemically negative relative to the aluminum matrix and will dissolve readily in the presence of an electrolyte such as saltwater. Thus, the presence of grain boundary β phase would add a second possible cracking mechanism, i.e., anodic dissolution mechanism. It is speculated that an anodic dissolution mechanism would operate in parallel with a hydrogen embrittlement mechanism for fully sensitized Al 5083 in saltwater, and might even be a dominant cracking mechanism at high stress ratio of R = 0.85. The exceptionally low ΔK_{th} of fully sensitized Al 5083 observed at R = 0.85 in 1% NaCl solution can be explained by the interplay between cyclic corrosion fatigue and static stress-corrosion cracking and will be discussed further later.

EFFECT OF [NaCl] CONCENTRATION ON HIGH STRESS-RATIO CORROSION FATIGUE

The effect of [NaCl] concentration on high stress ratio (R = 0.85) fatigue crack growth of fully sensitized Al 5083 is shown in Fig. A-6. As shown in Fig. A-6, the fatigue crack growth rates in diluted saltwater (0.001 and 0.01 wt% NaCl) are comparable and are the slowest. The fatigue crack growth rates increase rapidly when [NaCl] increases from 0.01 to 1%. Above 1% [NaCl], the fatigue crack growth rates stop increasing as the crack growth rates are essentially the same in 1% and in 15% [NaCl]. Correspondingly, the ΔK_{th} in 0.001 and 0.01 wt% are comparable, as shown in Fig. A-6b. Above 0.01 wt% [NaCl], the ΔK_{th} decreases rapidly until [NaCl] of 1 wt%. Above 1 wt%, the ΔK_{th} only decreases slightly as [NaCl] increases from 1 to 15 wt%.

EFFECT OF LOAD RATIO

The effects of load ratio on fatigue crack growth of as-received Al 5083-H131 and fully sensitized Al 5083 in 1% NaCl solution are shown, respectively, in Figs. A-7a and A-7b. The load ratios selected range from R = 0.1 to R = 0.85. As shown in Fig. A-7, the fatigue crack growth rates are higher at higher stress ratio for both alloys, except the fatigue crack growth curves of fully sensitized Al 5083 are shifting toward lower stress intensities at high stress ratios (R = 0.7 and 0.85) as shown in Fig. A-7b.

The effects of load ratio on ΔK_{th} are shown in Fig. A-8 for both as-received and fully sensitized Al 5083 in 1% NaCl solution. As shown in Fig. A-8, ΔK_{th} decreases with increasing load ratio from R = 0.1 to R = 0.7. Above R = 0.7, the ΔK_{th} remains unchanged for as-received Al 5083-H131. For fully sensitized Al 5083, the ΔK_{th} decreases further as the stress ratio increases from R = 0.7 to R = 0.85, and reaches a very low value of 0.45 MPa$\sqrt{m}$. This further drop in ΔK_{th} at R = 0.85 for fully sensitized Al 5083 in 1% NaCl solution is due to stress-corrosion cracking as the maximum stress

intensity during the fatigue cycle at such high stress ratio is above the stress-corrosion cracking threshold (K_{1SCC}).

EFFECT OF SENSITIZATION ON STRESS-CORROSION CRACKING RESISTANCE

The effect of aging time (at 175°C) on the stress-corrosion cracking resistance of Al 5083-H131 in 1% NaCl solution is shown in Fig. A-9. As shown in Fig. A-9, the K_{1SCC} decreases rapidly upon aging at 175°C. The K_{1SCC} for as-received Al 5083-H131, where there is no β on the grain boundaries, is about 27 MPa√m, while the K_{1SCC} for the fully-sensitized Al 5083 (such as 175 C/240 hrs), where the grain boundaries are covered by a continuous β film, is only 1.9 MPa√m. Further aging beyond 240 hours at 175°C leaves the K_{1SCC} essentially unchanged and it remains low at about 2 MPa√m. Since the fracture paths under SCC and corrosion-fatigue conditions are intergranular, the β facilitates crack growth by a dissolution mechanism. In addition, hydrogen evolves during the dissolution process and hydrogen thus generated could also migrate to the crack tip region and aid crack growth through a hydrogen embrittlement mechanism. Thus, the higher corrosion-fatigue crack growth rates and lower ΔK_{th} in the sensitized Al 5083 can be attributed to the presence of grain boundary β. Even small amounts of discontinuous β on the grain boundary degrades the SCC and fatigue properties relative to as-received condition, and is most damaging if the β is continuous.

EFFECT OF [NaCl] CONCENTRATION ON STRESS- CORROSION CRACKING RESISTANCE

The effect of [NaCl] concentration on stress-corrosion cracking resistance of fully sensitized Al 5083 is shown in Fig. A-10. As shown in Fig. A-10, the stress-corrosion cracking threshold stress intensity, K_{1SCC}, in diluted saltwater (0.001 and 0.01 wt% NaCl) are comparable and are about 24 MPa√m. The K_{1SCC} and the SCC resistance decrease rapidly when [NaCl] increases from 0.01 to 1%. Above 1% [NaCl], the K_{1SCC} stops increasing as the K_{1SCC} are essentially the same in 1% and in 15% [NaCl]. Data in Fig. A-10 suggests that a minimum [NaCl] concentration, which is above 0.01%, is required for the grain boundary β phase in fully sensitized Al 5083 to dissolve, and thus reduce the alloy's SCC resistance. This suggestion is supported by the SEM fractographic examinations and will be discussed later.

THE RELATION BETWEEN SCC AND CORROSION FATIGUE

The relation between K_{1SCC} and ΔK_{th}, using a two-parameter (K_{MAX} - ΔK) approach, is presented in Fig. A-11.

The high stress-ratio CF and SCC response of Al 5083 can be analyzed using a superposition model and a two-parameter approach to environment-assisted cracking. The superposition model is essentially a summation of independent terms for inert environment cracking behavior, a cyclic corrosion-fatigue behavior, and an intrinsic stress corrosion cracking behavior:

$$(da/dN)_{Total} = (da/dN)_{Inert} + (da/dN)_{CF} + (da/dN)_{SCC}$$

At threshold, all three terms must be separately zero. In the present case, the "inert" term can be ignored because the threshold in vacuum is much higher than in the 1% NaCl, leaving the separated terms for corrosion-fatigue, characterized by a cyclic-only fatigue threshold that we term ΔK_{CFTH}, and stress-corrosion cracking, which is characterized by a threshold for K_{MAX}, that is, K_{1SCC}. Physically, this simply means that a crack won't grow when two conditions are met simultaneously: the peak stress intensity is less than K_{1SCC}, *and* the cyclic stress intensity is below ΔK_{CFTH}, as shown in Fig.11, in the region to the left and below the curve "ABC". The crack will grow in the region to the right and above the "ABC" curve, when CF stress intensity is above ΔK_{CFTH} and/or K_{max} is above K_{1scc}.

For high stress-ratio of R = 0.85 used in this study, one can draw a trajectory line corresponding to R = 0.85, based on a two-parameter approach" as shown in Fig. A-11. In as-received Al 5083-H131 in 1% NaCl, the K_{1SCC} = 27 MPa√m line intersects the R = 0.85 line way above the curve "ABC", and thus, SCC does not contribute to crack growth as the cyclic K_{MAX} is below K_{1SCC}. When Al 5083 is partially sensitized at 175 °C/50 hrs, K_{1SCC} = 9 MPa√m and this K_{1scc} line also intersects the R = 0.85 line above the "ABC" curve. This suggests SCC does contribute to crack growth when the cyclic K_{MAX} is greater than 9 MPa√m. However, at near ΔK_{CFTH}, the cyclic K_{MAX} is smaller than K_{1SCC} = 9 MPa√m, and, hence, does not contribute to crack growth and the crack grows by a CF mechanism. As the sensitization deepens, as in the case of 175 °C/100 hrs, the K_{1SCC} = 6 MPa√m line intersects the R = 0.85 line below the "ABC" curve. This indicates that, above the "ABC" curve, both CF and SCC are operating. But below the "ABC" curve, though it is in the region where no corrosion fatigue cracking should take place, K_{MAX} during corrosion fatigue, however, is higher than K_{1scc} and, thus, cracks will grow because of SCC. The measured ΔK_{TH} = 0.92 MPa√m is, therefore, an apparent threshold resulting solely from the SCC contribution. In fully sensitized Al 5083 (175 °C/240 hrs), the $K_{1SCC} \approx$ 3 MPa√m line intersects the R = 0.85 line and gives the apparent ΔK_{TH}, which is (1- R) x K_{1SCC} = 0.45. This predicted value agrees well with the measurements, and is well below the cyclic-only threshold, $\Delta K_{CFTH} \approx$ 1 MPa√m. Here, the *apparent* ΔK threshold resulting from the SCC contribution is much less than the cyclic fatigue-only threshold ΔK_{CFTH}. The above discussion demonstrates that the relation between high stress-ratio CF and SCC can be quantitatively established.

TWO-PARAMETER (K_{MAX} - ΔK) APPROACH FOR ENVIRONMENTAL EFFECT

The two-parameter K_{MAX} - ΔK approach that has been used successfully to explain the relation between K_{1SCC} and ΔK_{th} in partially sensitized Al 5083 also can be used to account for the observed environmental sensitivity in fully sensitized Al 5083. A two-parameter diagram is shown in Fig. A-12. As shown in Fig. A-12, the L-curves corresponding to vacuum and NaCl environments are drawn in green and blue, respectively. Trajectories corresponding to R = 0.1 and R = 0.85 are also drawn in Fig. A-12. In this two-parameter presentation, the region to the right of and above the L-curve is the "Crack Growth Region", because the ΔK and K_{max} are greater than ΔK_{CFth} and

K_{MAXth}. The "green" and the "red" dots shown in Fig. A-12 are actually data points derived from ΔK_{th} obtained in each environment. Under high stress-ratio of R = 0.85, as the test environment becomes more aggressive, the ΔK_{th} decreases following the "R = 0.85" trajectory. As shown in Fig. A-12, the ΔK_{th} for air, 0.001 wt% NaCl, and 0.01 wt% NaCl closely group together and near the "Blue NaCl" L-curve, indicating [NaCl] concentration below 0.01 wt% does not enhance corrosion-fatigue crack growth. Above [NaCl] concentration of 0.01 wt%, however, ΔK_{th} decreases quickly until [NaCl] concentration reaches 1 wt%. Above 1 wt% [NaCl], the environmental effect becomes saturated and ΔK_{th} only decreases slightly between 1 and 15 wt% [NaCl]. These observations are consistent with the "Superposition of CF and SCC Model", as the vertical lines corresponding to $K_{MAX} = K_{1SCC}$ intersect R = 0.85 trajectory below the "Blue NaCl" L-curve.

SEM FRACTOGRAPHIC EXAMINATION

The fracture surface morphology of the fatigue-fractured specimens was examined by scanning electron microscopy (SEM) and is briefly summarized in Table B-1. In inert vacuum environment, the fracture paths are transgranular in all cases, irrespective of the aging conditions and load ratios. On the other hand, at a high stress ratio of R = 0.85 in 1% NaCl solution, the fracture paths are intergranular for both as-received and aged Al 5083. Figures A-13 and A-14 show examples of intergranular fracture surface morphologies of Al 5083-H131 and sensitized Al 5083 tested in 1% NaCl solution at either R = 0.1 (Fig. A-13) or R = 0.85 (Fig. A-14) taken from the low stress intensity regions. At higher magnification, numerous Mn- and Cr-rich particles can be seen on these grain boundaries, as shown in Fig. A-15. These observations suggest that, in 1% NaCl solution, under a high stress ratio (and in the low stress intensity region of load stress ratio), grain boundaries are favored fracture paths, with and without the presence of β phase on the grain boundaries. In a less aggressive ambient air environment, the fracture surface morphology consists of a mixture of both transgranular and intergranular features.

As shown in Table B-1 and in Figures A13 – 15, the fracture paths are intergranular for sensitized Al 5083 fatigued in 1% NaCl solution. Since, in sensitized Al 5083, the grain boundaries are covered with continuous thin β phase film (~ 100 nm thick), an outstanding question is in such case does the fracture path follow the interface between β phase and the Al 5083 grain boundary or is the fracture path through the β phase? Unfortunately, it is difficult if not impossible to answer the above question. It is because the β phase is highly anodic relative to the aluminum matrix and dissolves completely in saltwater solution. Thus, in post-fracture matching surface analyses, β is gone and the evidence to delineate whether the fracture path follows the β/Al grain boundary or through β phase is no longer there.

The stress-corrosion cracking fracture surface morphologies of sensitized Al 5083S in various concentrations of [NaCl] are shown in Fig. A16. As shown in Figs. A-16a and A-16b, the fracture mode immediately ahead of the fatigue precrack in 0.001 and 0.01% NaCl solutions are transgranular ductile void coalescences. This observation suggests the

lack of environmental attack in these very dilute [NaCl] solutions. It is speculated that the β phases in the sensitized Al 5083S are not dissolved in these dilute solutions and, hence, the K_{1SCC} are very high. The ductile void coalescence fractures are the result of sustained-load cracking. On the other hand, as shown in Figs. A16c and A-16d, the fracture paths change to completely intergranular when [NaCl] is higher than 0.1%. This suggests that β phase along the grain boundaries of sensitized Al 5083S is dissolved and the stress-corrosion cracking causes very low K_{1SCC} in these environments. These SEM fractographic examinations agree well with the K_{1SCC} data shown in Fig. A-7.

Fig. A-17 shows the high stress-ratio corrosion-fatigue cracking fracture surface morphologies in the near-threshold regions of sensitized Al 5083S in various concentrations of [NaCl]. As shown in Figs. A-17a and A-1b, the fracture mode in 0.001 and 0.01% NaCl solutions are transgranular, which is typical for fatigue fracture of aluminum alloys in benign environments. This observation suggests the lack of environmental attack in these very dilute [NaCl] solutions and is associated with high fatigue crack thresholds. However, as shown in Figs. A17c and A-17d, the fracture paths change to completely intergranular when [NaCl] is higher than 0.1%, and this type of fracture is associated with low corrosion-fatigue crack thresholds. The fractographic results under corrosion-fatigue conditions, as shown in Fig. A-17, are somewhat similar to that under stress-corrosion cracking, as shown in Fig. A-16. Again, the major reason for the low corrosion-fatigue cracking threshold seen in higher [NaCl] concentrations is the dissolving of grain boundary β phases in these environments. These SEM fractographic examinations agree well with the ΔK_{th} data shown in Fig. A-6.

CONCLUSIONS

The effect of sensitization on the stress-corrosion cracking (SCC) and corrosion-fatigue (CF) cracking resistance of Al 5083 is investigated. The as-received Al 5083-H131 was sensitized by aging at 175 °C for 1 – 4000 hours. Previous TEM studies indicated that while the as-received Al 5083-H131 has no β phase on the grain boundaries, isolated islands of β starts to form on the grain boundaries after aging at 175 °C for as short as one hour. Between 1 and 240 hours, a more complex structure, yet discontinuous, β forms on the grain boundaries. After sufficiently long aging times, the β forms a continuous film on the grain boundaries.

While the presence of β phase on the grain boundaries of fully sensitized Al 5083 does not affect the corrosion-fatigue cracking resistance in vacuum, ambient air, and at low stress ratios in saltwater, it is detrimental to saltwater high stress-ratio corrosion fatigue properties, significantly increasing corrosion-fatigue crack growth rates and lowering ΔK_{th}. When grain boundary β is discontinuous (less than 240 hour aging at 175 °C), the increase in corrosion-fatigue crack growth rates and decrease in ΔK_{th} are linearly related to the aging time and thus directly correlated to the amount of discontinuous β on the grain boundaries. When grain boundaries are covered by a continuous β film upon prolonged aging (> 240 hours), corrosion-fatigue crack growth rates reach a maximum and ΔK_{th} a minimum and remain unchanged with further aging.

Similarly, the presence of grain boundary β, even discontinuous, significantly reduces the SCC resistance of Al 5083. When Al 5083 is fully sensitized and the grain boundaries are covered with continuous β film (greater than 240 hour aging at 175 °C), the SCC threshold (K_{1scc}) reaches a minimum and is less than an order-of-magnitude of unsensitized Al 5083-H131 (2 vs. 28 MPa√m).

The relation between K_{1scc} and high stress-ratio ΔK_{th} can be illustrated graphically using a "K_{max} - ΔK" two-parameter approach. This relation suggests that the low apparent ΔK_{th} in fully sensitized and partially sensitized Al 5083 can be predicted from their respective K_{1scc} and the applied stress ratio.

The effects of saltwater concentration, [NaCl], on K_{1scc} and ΔK_{th} of fully sensitized Al 5083, with [NaCl] ranging from 0.001 to 15 wt% were investigated. At [NaCl] below 0.01 wt%, K_{1scc} and ΔK_{th} are high and are not affected by [NaCl]. Above [NaCl] of 0.01 wt%, however, both K_{1scc} and ΔK_{th} decrease rapidly within one or two orders-of-magnitude increase in [NaCl].

REFERENCES

1. J.L. Searles, P.I. Gouma, R.G. Buchheit, Metall. Mater. Trans. A 32A, 2859 (2001).

2. F.S. Bovard, in *Corrosion in Marine and Saltwater Environments II*, Electrochemical Society Proc., D.A. Shifler, T. Tsuru, P.M. Natishan, and S. Ito, eds., Electrochemical Society, vols. 2004-2014, 232 (2005).

3. R. Goswami, G. Spanos, P.S. Pao, R.L. Holtz, Mater. Sci. Eng. A 527, 1089 (2010).

4. R. Goswami, G. Spanos, P.S. Pao, R.L. Holtz, Metall. Mater. Trans. A, in press (2010).

5. M. Popovic and E. Romhanji, Mater. Sci. Eng. A, 492, 460 (2008).

6. M.C. Carroll, P.J. Gouma, M.J. Mills, G.S. Daehn, B.R. Dunbar, Scripta Mater. 42, 335 (2000).

7. H. Yukawa, Y. Murate, M. Morinaga, Y.Takahashi, H. Yoshida, Acta Metal. Mater. 43, 681 (1995).

8. I.N.A. Oguocha, O.J. Adigun, S. Yannacopoulos, J. Mater. Sci. 43, 4208 (2008).

9. J.L. Searles, P.J. Gouma, R.G. Buchheit, Mater. Sci. Forum 396-402, 1437 (2002).

10. T.D. Burleigh, Corrosion 47, 89 (1991).

11. R.H. Jones, D.R. Baer, M.J. Danielson, and J.S. Vetrano, Metall. Mater. Trans. A 32A, 1699 (2001).

12. Ashok Saxena and S.J. Hudak, Jr., Int. J. Fract., 1978, Vol. 14, pp. 453-468.

13. *Standard Test Method for Plane-Strain Fracture Toughness of Metallic Materials, ASTM E 399-06*, ASTM International, (2006).

14. R.P. Wei, P.S. Pao, R.G. Hart, T.W. Weir, and G.W. Simmons, "Fracture Mechanics and Surface Chemistry Studies of Fatigue Crack Growth in an Aluminum Alloy," *Metall. Trans. A.* Vol. 11A, 1980, pp. 151-158.

15. A. Bonakdar, F. Wang, J.J. Williams, and N. Chawla, "Environmental Effects on Fatigue Crack Growth in 7075 Aluminum Alloy," *Metall. Mater. Trans. A*, Vol 43A, 2012, pp. 2799-2809.

16. P.P. Wei and R.P. Gangloff, Fracture Mechanics: Perspectives and Directions, ASTM STP 1020,R.P. Wei and R.P. Gangloff, eds., ASTM Philadelphia, PA 1989, pp. 233-264.

17. A. Hartman, Int. J. Fracture, 1965, Vol.1, pp. 167-188.

18. P.S. Pao, Ming Gao, and R.P. Wei, Scripta Metall., 1985, Vol. 19, pp. 265-270.

APPENDIX A
FIGURES

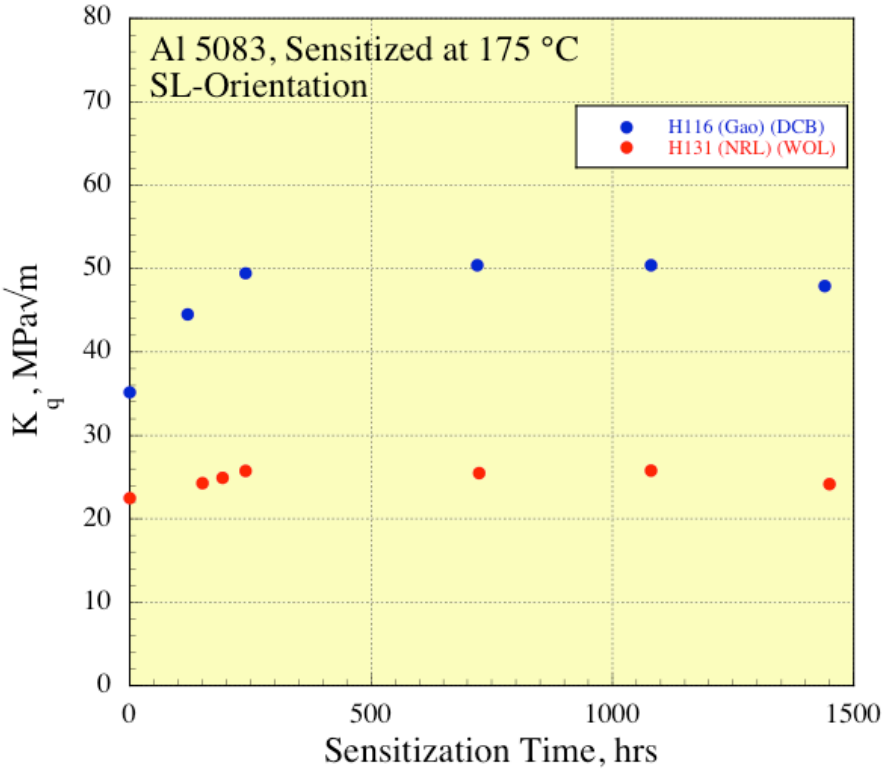

Figure A-1: Effect of sensitization time at 175°C on fracture toughness of Al 5083.

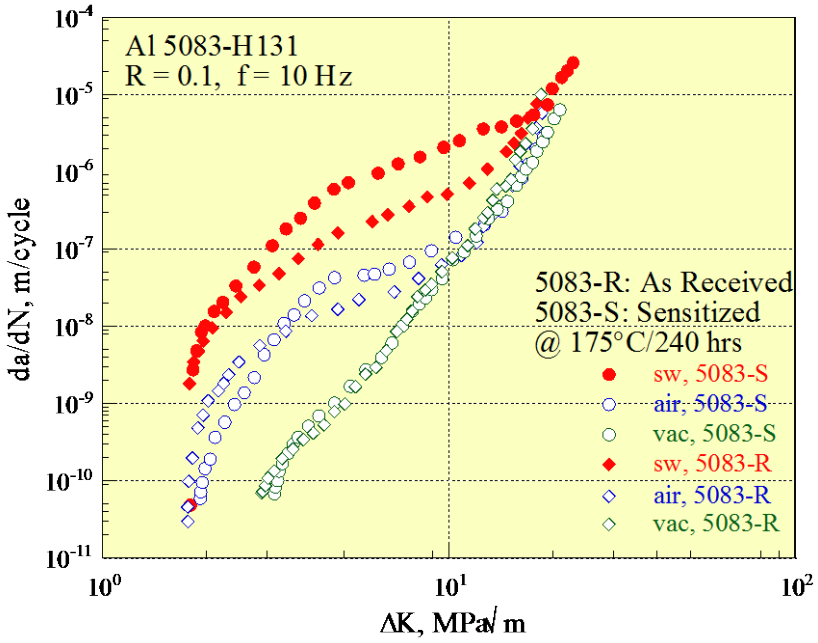

(a)

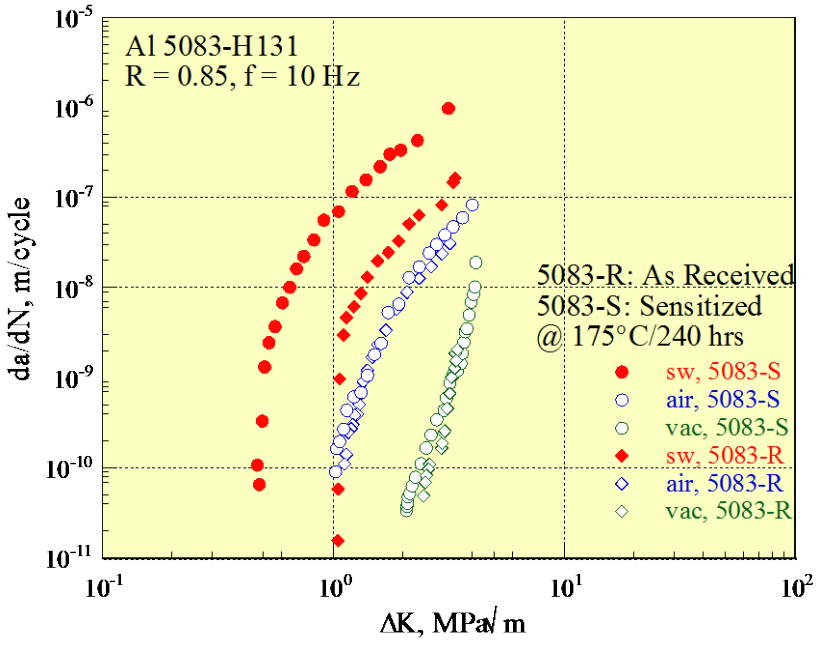

(b)

Figure A-2: Comparison of fatigue crack growth of as-received Al 5083 and sensitized Al 5083 in vacuum, ambient air, and 1% NaCl at (a) R = 0.1 and (b) R = 0.85.

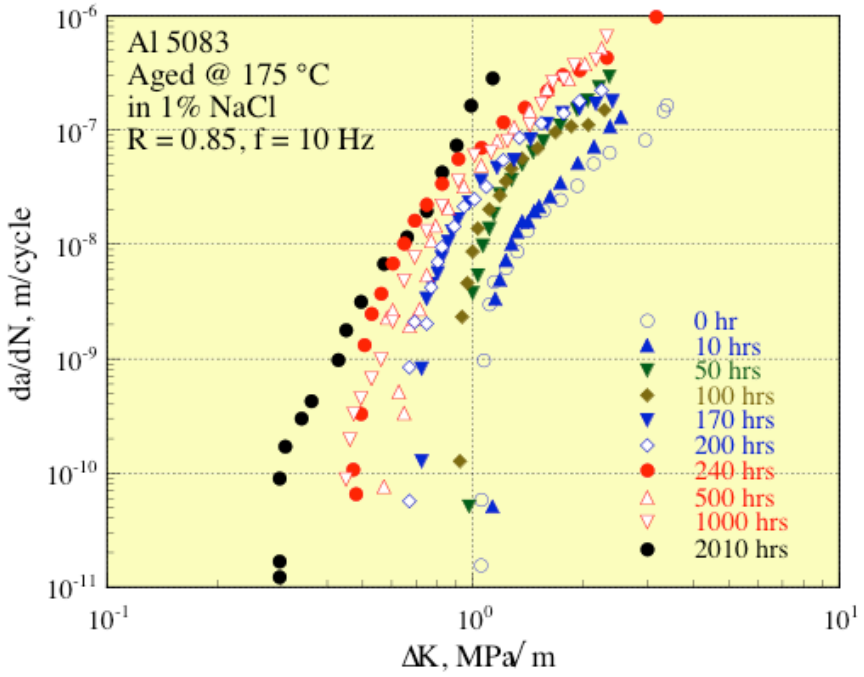

Figure A-3: Effect of sensitization time at 175°C on fatigue crack growth kinetic of Al 5083 at R = 0.85 in 1% NaCl solution.

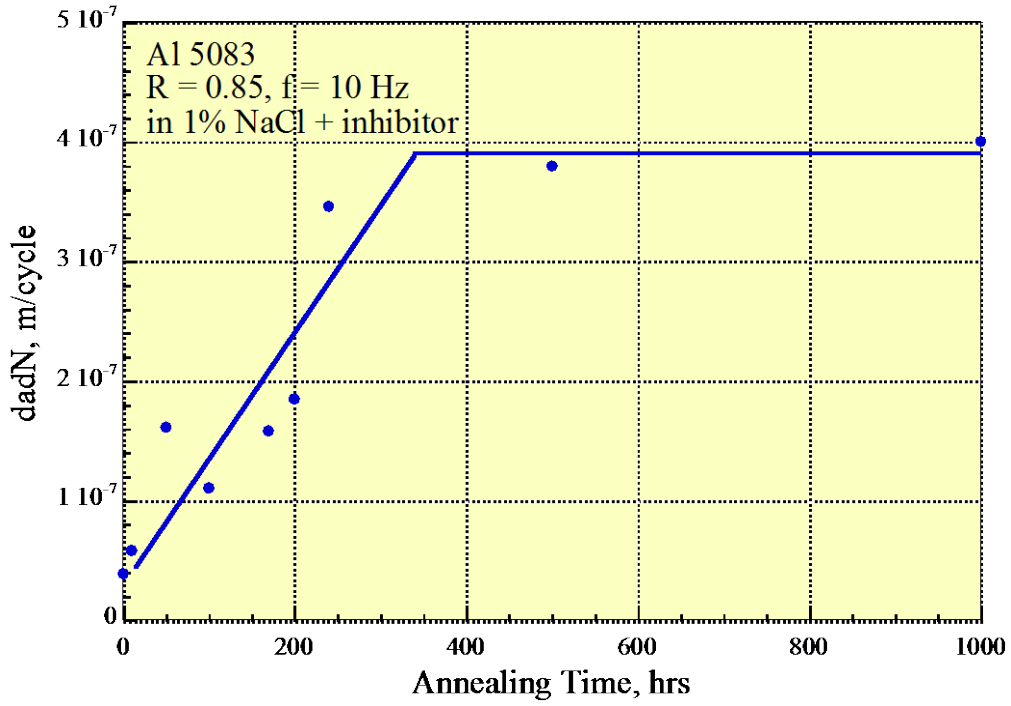

Figure A-4. Effect of aging on the fatigue crack growth rate at $\Delta K = 2$ MPa$\sqrt{m}$ of Al 5083 in 1% NaCl solution at a stress ratio of 0.85.

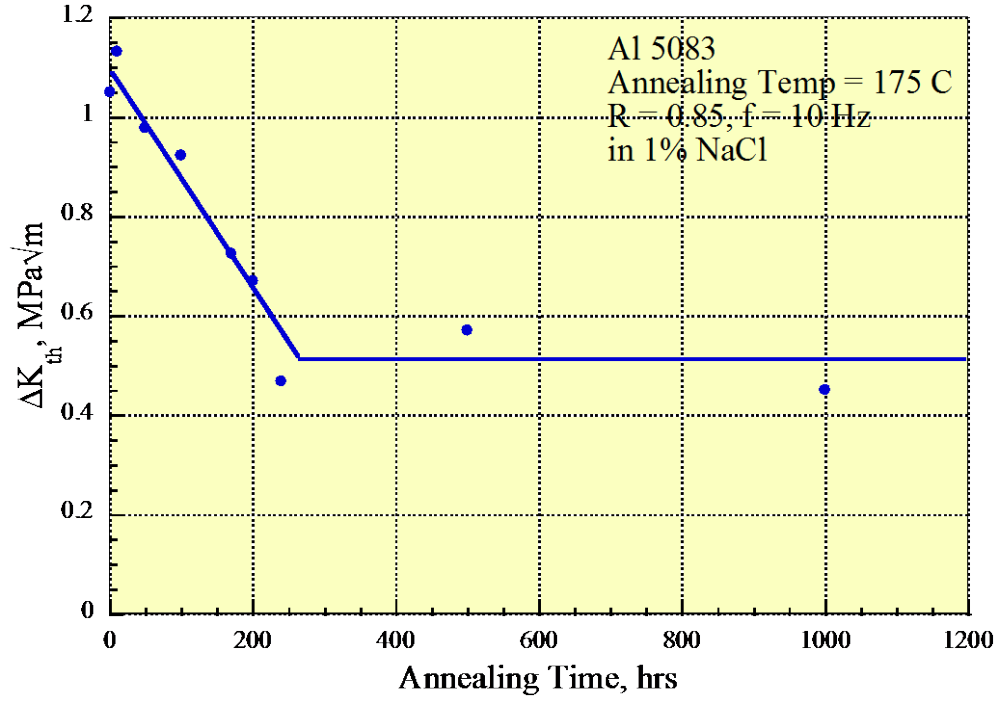

Figure A-5. Effect of aging on the fatigue crack growth threshold stress intensity of Al 5083 in 1% NaCl solution at a stress ratio of 0.85.

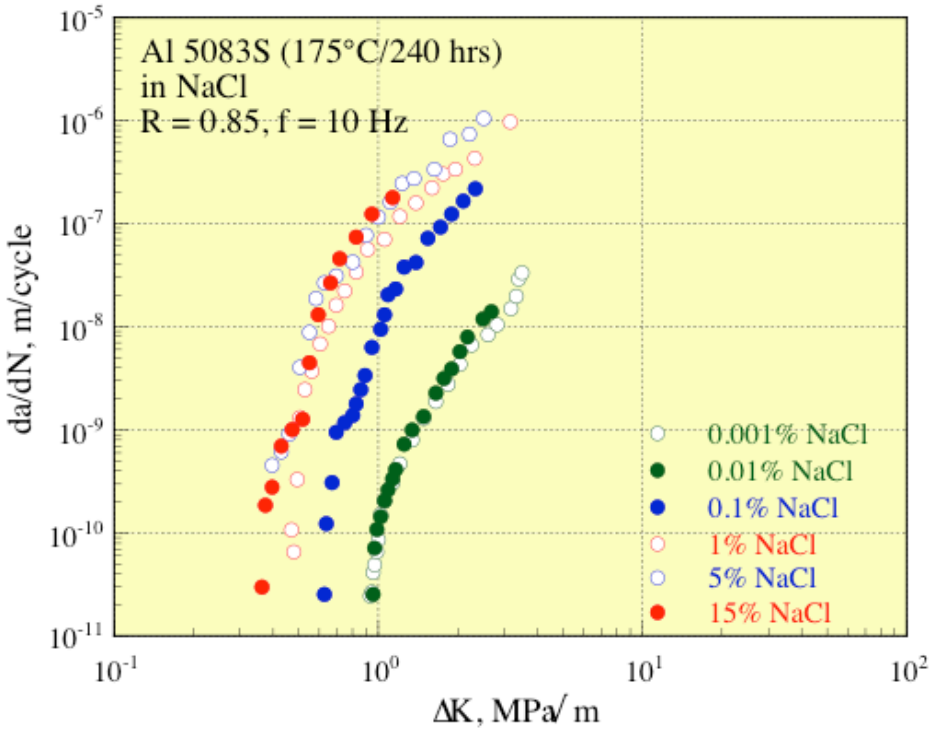

(a)

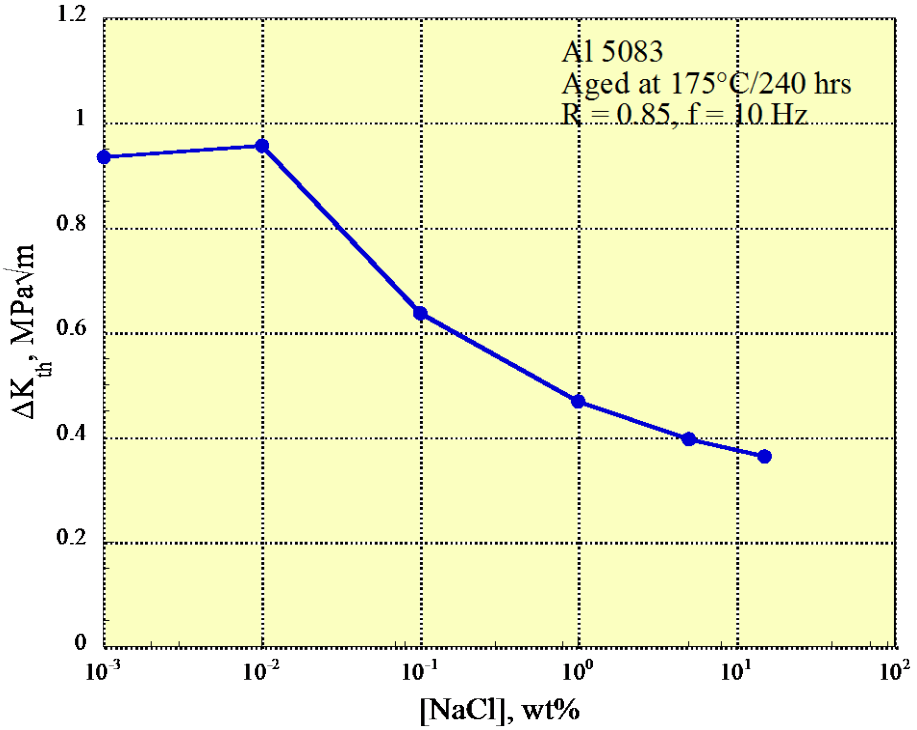

(b)

Figure A-6: Effect of [NaCl] concentration on (a) fatigue crack growth kinetic and (b) ΔK_{th} of sensitized Al 5083 (175°C/240 hrs) at R = 0.85.

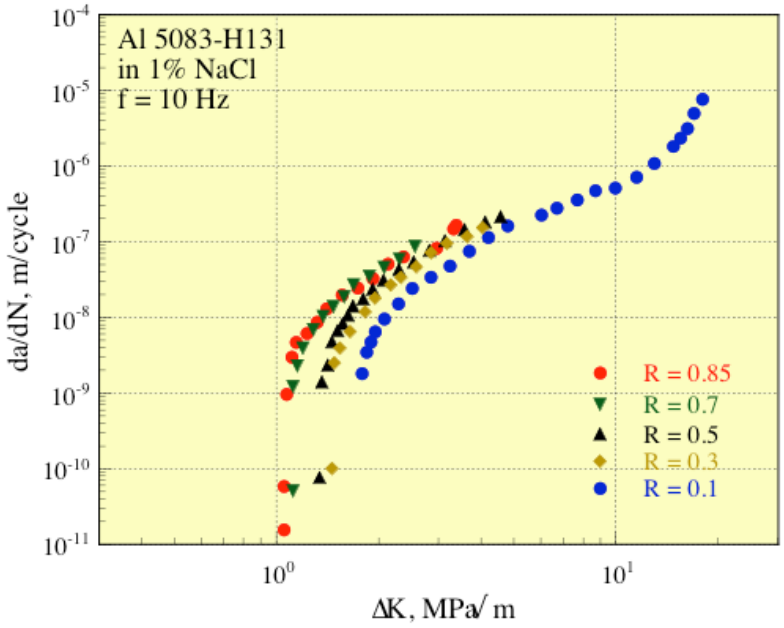

(a)

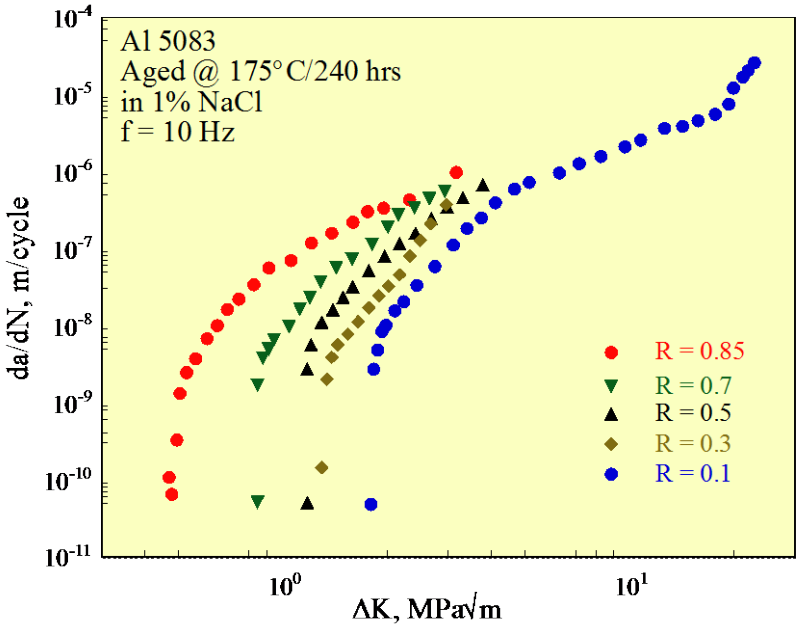

(b)

Figure A-7: Effect of load ratio on fatigue crack growth in 1% NaCl solution of (a) as-received and (b) sensitized (175°C/240 hrs) Al 5083.

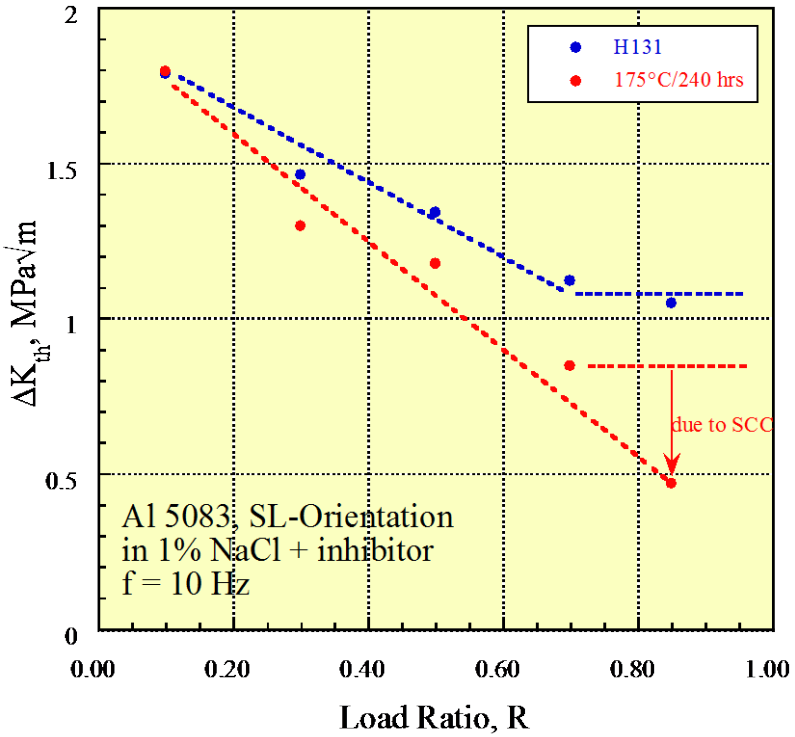

Figure A-8: Effect of load ratio on ΔK_{th} of as-received and sensitized (175°C/240 hrs) Al 5083.

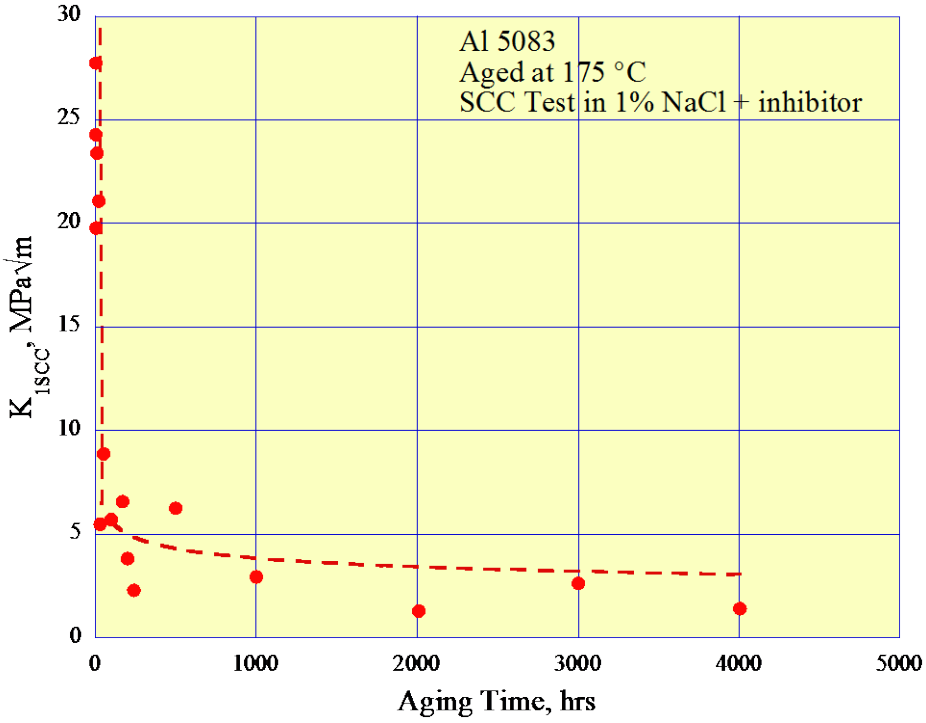

Figure A-9: Effect of aging time at 175°C on stress-corrosion cracking threshold (K_{1SCC}) of Al 5083 in 1% NaCl.

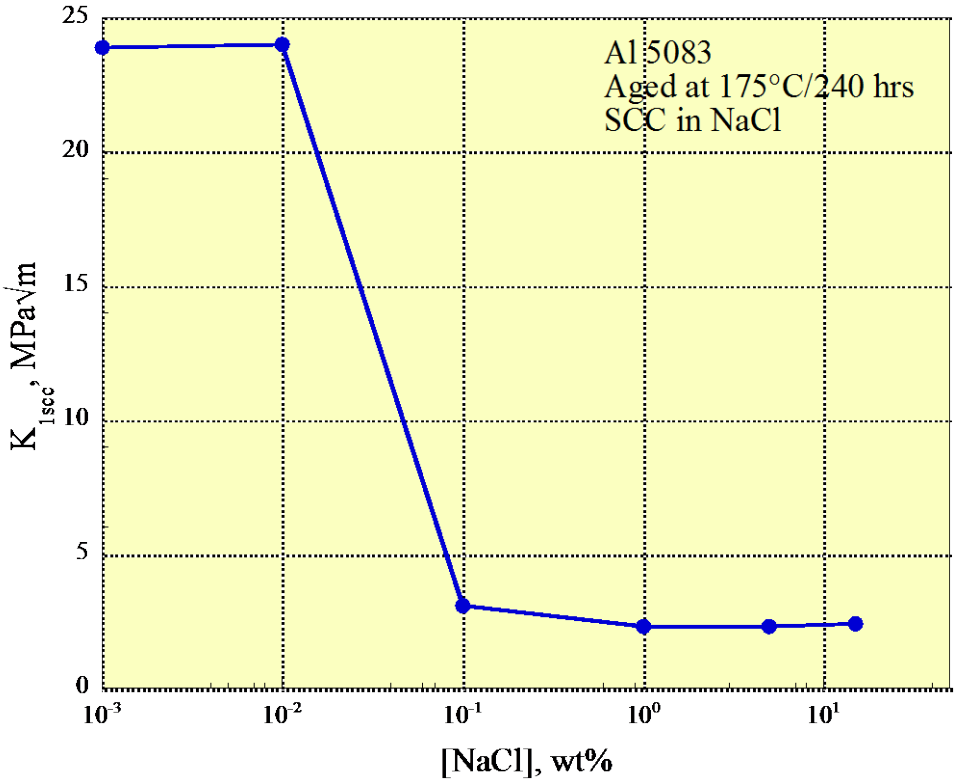

Figure A-10: Effect of [NaCl] concentration on K_{1SCC} of sensitized Al 5083 (175°C/240 hrs).

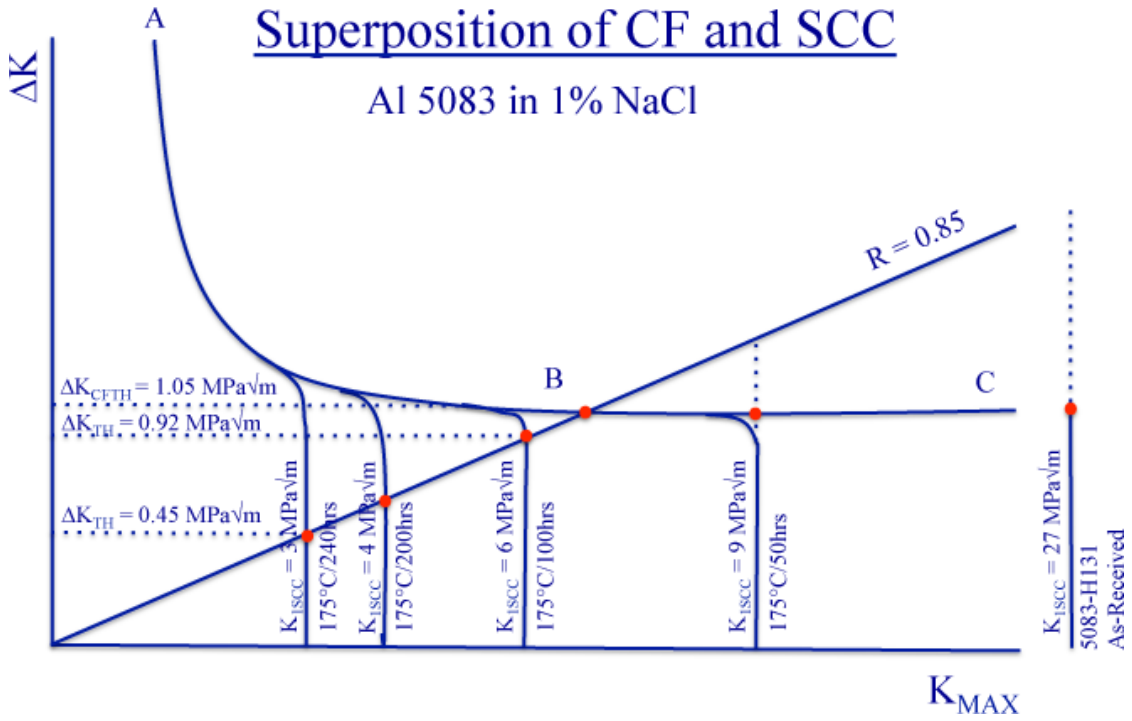

Figure A-11: Schematics illustrates the relation between high stress-ratio CF and SCC, using a two-parameter "K_{MAX} - ΔK" approach. With increased sensitization, the intersection of the K_{1SCC} line and the R = 0.85 line, that is, the apparent corrosion-fatigue threshold, progressively decreases below ΔK_{CFTH}.

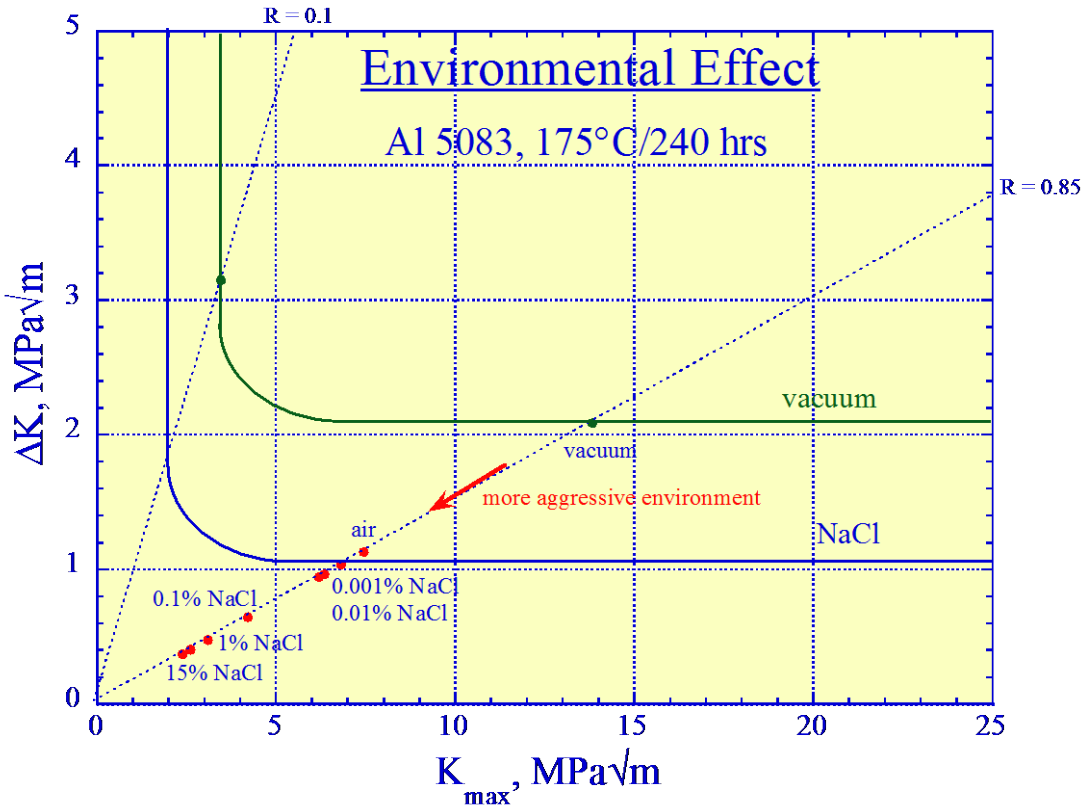

Figure A-12: Schematics illustrating the relation between high stress-ratio CF and SCC, using a two-parameter "K_{MAX} - ΔK" approach. When the test environment becomes more aggressive, ΔK_{th} progressively decreases following the R = 0.85 trajectory.

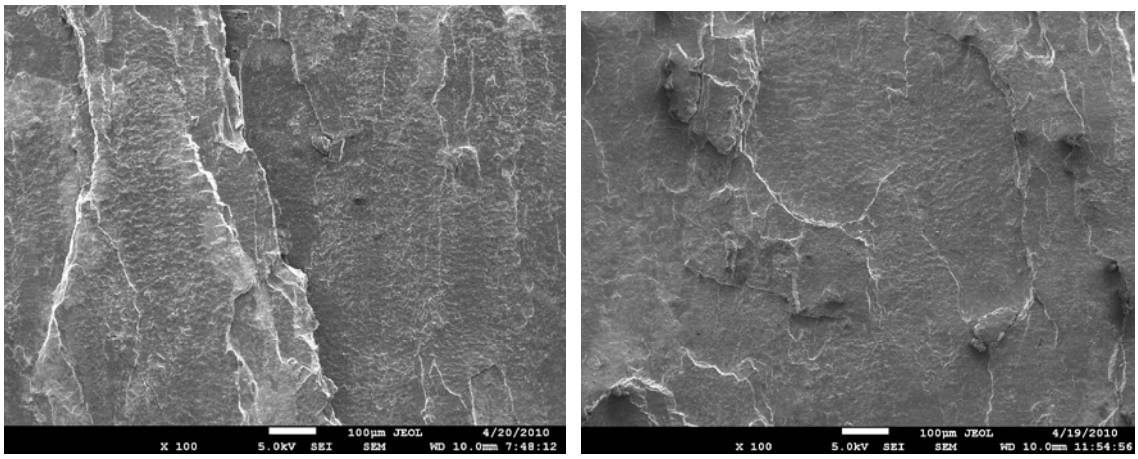

(a) (b)

Figure A-13: Comparison of fracture surface morphology of (a) Al 5083R (as-received) and (b) Al 5083S (sensitized at 175°C/240 hrs) fatigued at R = 0.1 in 1% NaCl solution in the near threshold region ($\Delta K = 2$ MPa$\sqrt{m}$ for both specimens).

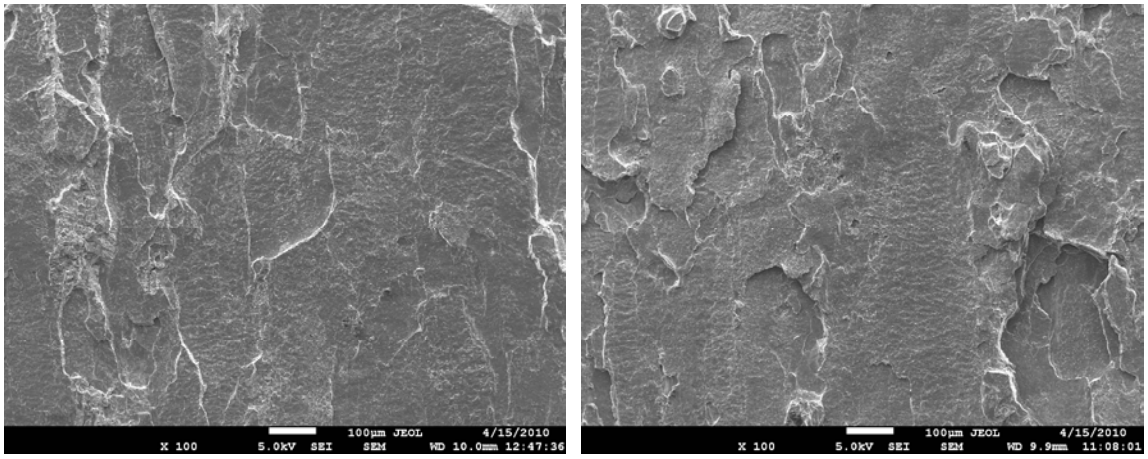

(a) (b)

Figure A-14: Comparison of fracture surface morphology of (a) Al 5083R (as-received) and (b) Al 5083S (sensitized at 175°C/240 hrs) fatigued at R = 0.85 in 1% NaCl solution in the near threshold region ($\Delta K = 1.1$ MPa$\sqrt{m}$ for Al 5083R and $\Delta K = 0.5$MPa$\sqrt{m}$ for Al 5083S).

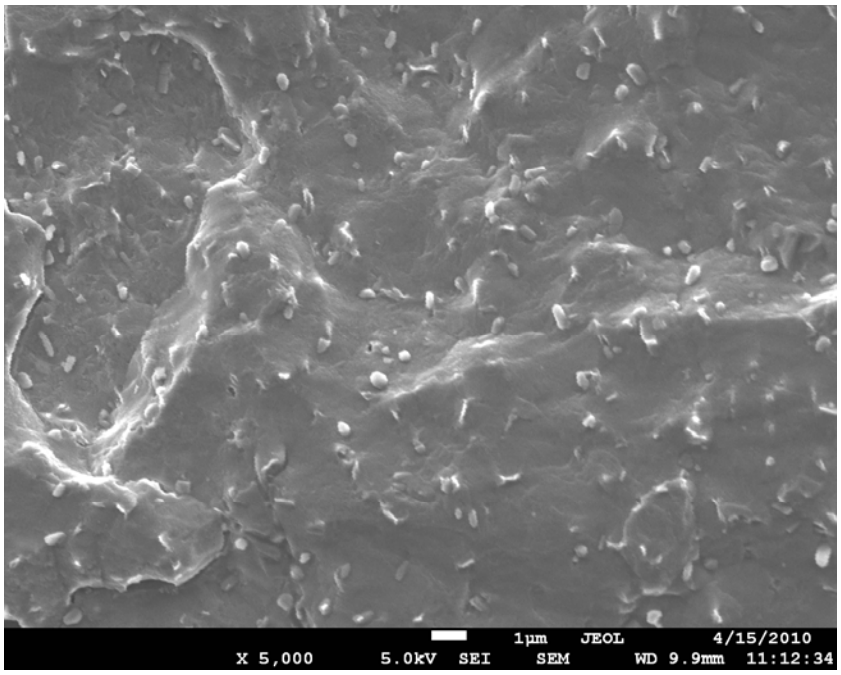

Figure A-15: High magnification fractograph in the near-threshold region ($\Delta K = 0.5$ MPa$\sqrt{m}$) of Al 5083 sensitized at 175°C/240 hrs tested at R = 0.85 in 1% NaCl solution.

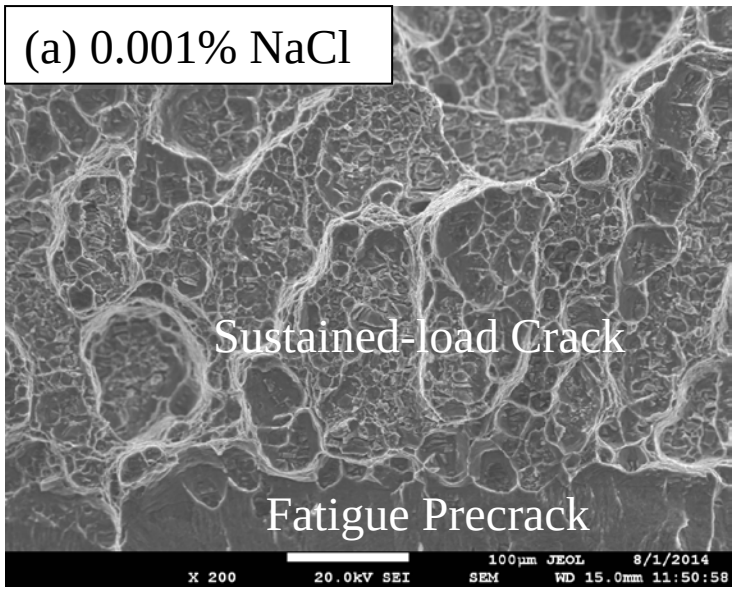
(a) 0.001% NaCl
Sustained-load Crack
Fatigue Precrack
X 200 20.0kV SEI SEM 100µm JEOL WD 15.0mm 8/1/2014 11:50:58

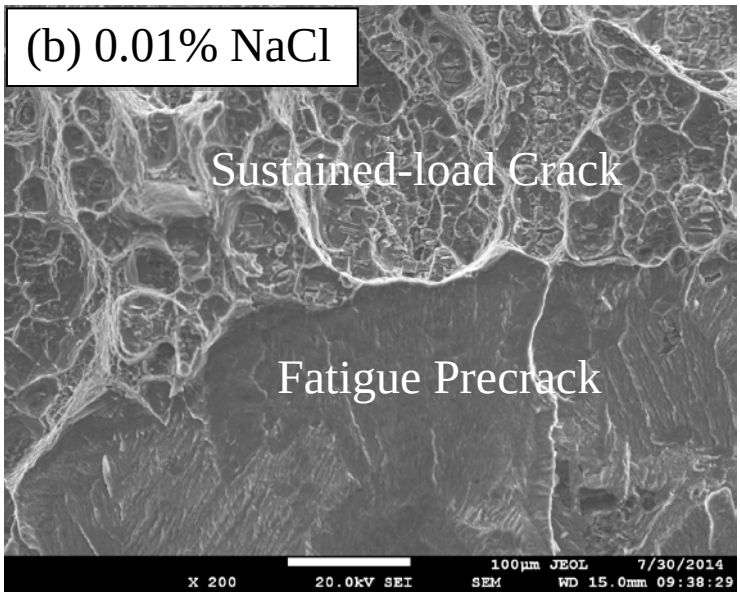
(b) 0.01% NaCl
Sustained-load Crack
Fatigue Precrack
X 200 20.0kV SEI SEM 100µm JEOL WD 15.0mm 7/30/2014 09:38:29

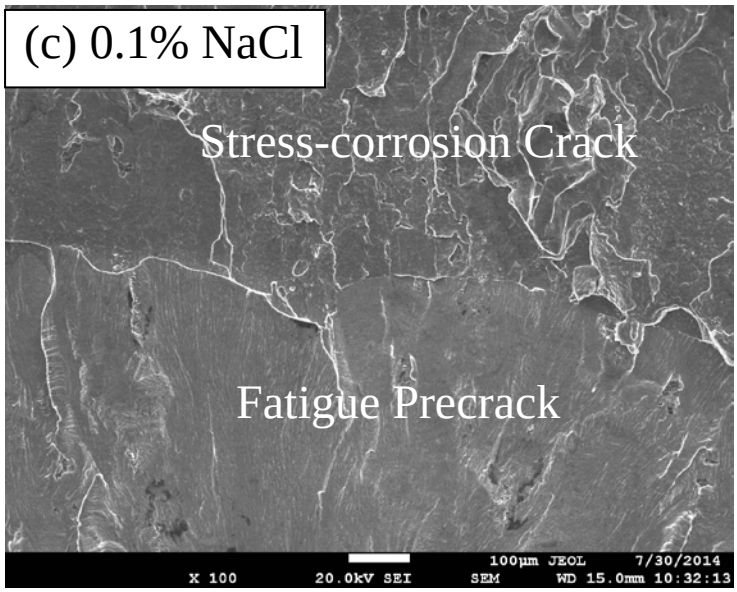

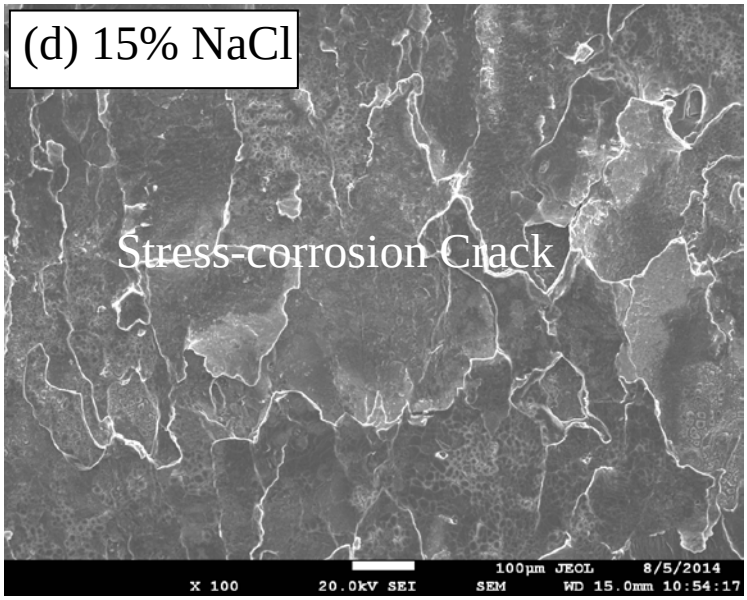

Figure A-16: Stress-corrosion cracking fracture surface morphologies of Al 5083 sensitized at 175°C/240 hrs tested in (a) 0.001% NaCl, (b) 0.01% NaCl, (c) 0.1% NaCl, and (d) 15% NaCl solution.

(a) 0.001% NaCl, ΔK = 0.97 MPa√m

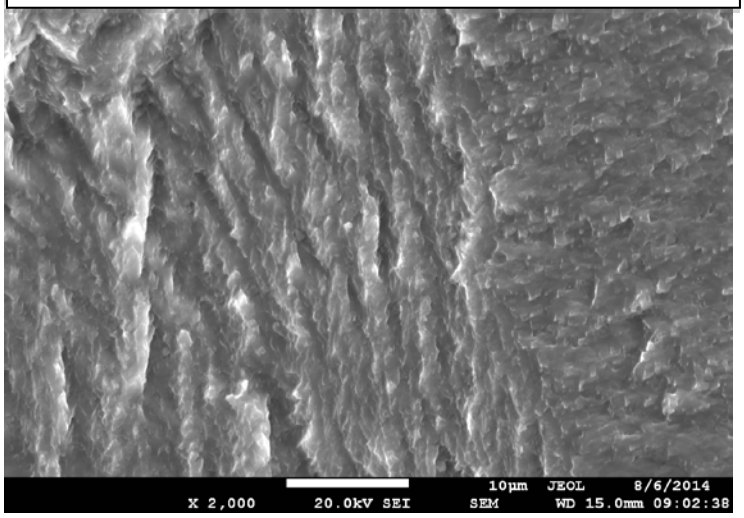

(b) 0.01% NaCl, ΔK = 0.98 MPa√m

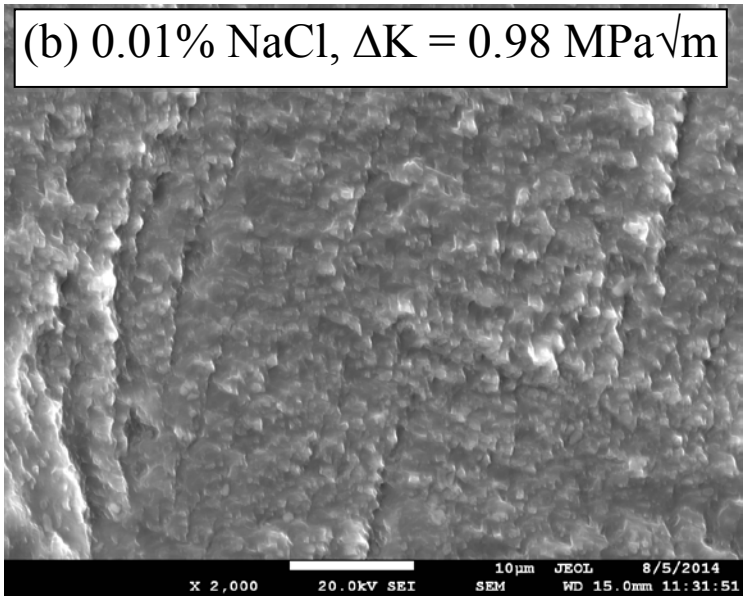

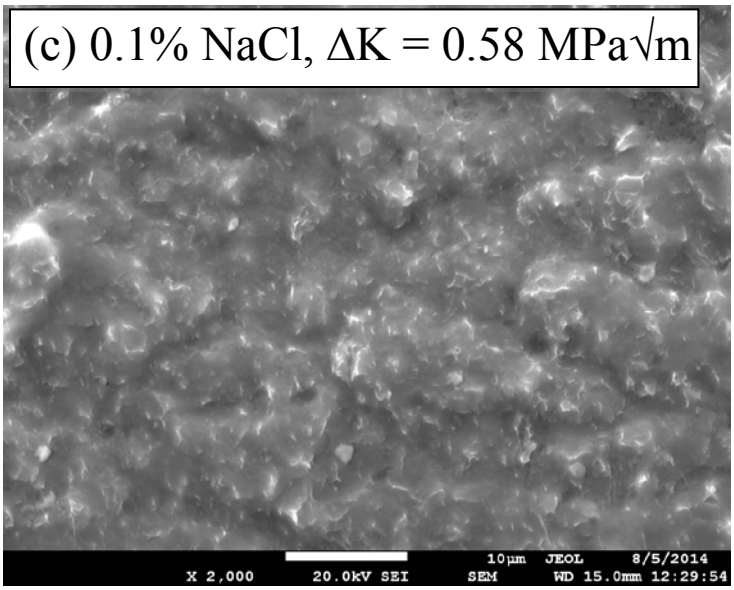

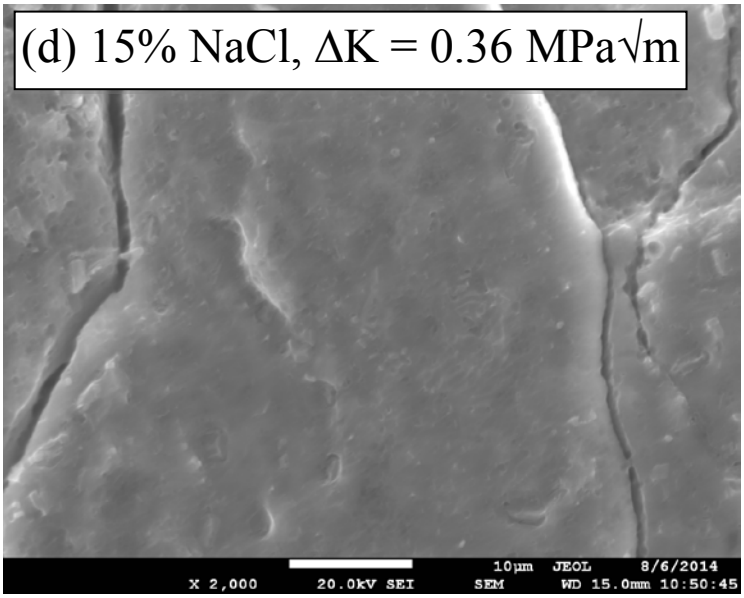

Figure A-17: Corrosion-fatigue cracking fracture surface morphologies of Al 5083 sensitized at 175°C/240 hrs tested in (a) 0.001% NaCl, (b) 0.01% NaCl, (c) 0.1% NaCl, and (d) 15% NaCl solution.

APPENDIX B
TABLE

Table B1: Al 5083 SEM Fractographic Analyses Summary

R	Environment	5083 Condition	Low	K Int	High
0.1	Vacuum	as-received	TG	TG	TG
		175°C/240h	TG	TG	TG
	Air	as-received	IG+TG	IG+TG	TG
		175°C/240h	IG+TG	IG+TG	TG striations
	Saltwater	as-received	IG	IG+TG	TG
		175°C/240h	IG	IG	TG
0.85	Vacuum	as-received	TG	TG	TG
		175°C/240h	TG	TG	TG
	Air	as-received	TG	IG+TG	IG+TG
		175°C/240h	TG	IG+TG	IG+TG
	Saltwater	as-received	IG	IG	IG
		175°C/170h	IG	IG	IG
		175°C/240h	IG	IG	IG
		175°C/1000h	IG	IG	IG